Evolution and Nucleosynthesis of Massive Stars and Related Nuclear Uncertainties

T. Rauscher[a]

[a]Departement für Physik und Astronomie,
Universität Basel,
CH-4056 Basel, Switzerland
E-mail: Thomas.Rauscher@unibas.ch

Properties of atomic nuclei important for the prediction of astrophysical reaction rates are reviewed. In the first part, a recent simulation of evolution and nucleosynthesis of stars between 15 and 25 $M_\odot$ is presented. This study is used to illustrate the required nuclear input as well as to give examples of the sensitivity to certain rates. The second part focusses on the prediction of nuclear rates in the statistical model (Hauser-Feshbach). Some of the important ingredients are addressed. Discussed in more detail are approaches to predict level densities, parity distributions, and optical α-nucleus potentials.

1. Introduction

The knowledge of nuclear reactions is crucial to model the evolution of stars and to determine the amounts of produced nuclei. From the abundance patterns of the elements we can learn something about how they were created and consequently it is possible to study the conditions in supposed astrophysical sites and, finally, to attempt to trace the origin and history of the Universe. An in-depth knowledge of the sub-atomic processes is required in order to understand many large-scale effects.

The demands of astrophysics challenge our ability to describe and predict nuclear properties and nuclear reactions. Due to high temperatures and densities in the stellar plasma, a large number of unstable nuclides are involved in the nucleosynthetic processes. Some of their radioactive decay lines can be observed by modern satellite observatories and provide an important tool to test the hydrodynamics of stellar models by comparison. However, this task can only be performed if the producing nuclear reactions are sufficiently well known. In this respect, not only reactions involving unstable targets are important but also such along the line of stability. Despite of temperatures in the range of millions to billions of Kelvin, the respective energies of the interacting particles are quite low by nuclear physics standards, from thermal energies up to a few MeV. Due to the size of the reaction networks (the nucleosynthesis calculations for massive stars, which are described below, include about 2400 nuclides in more than 15000 reactions), theoretical predictions will always remain important. However, the relevance of the low-energy region poses problems to both experimental and theoretical approaches. For neutron-induced reactions, to resolve the transition between and interplay of different reaction mechanisms – from direct

to resonant interactions and finally to the Hauser-Feshbach regime – remains a challenge. Except for activation experiments, standard techniques only measure the resonant part of the cross section. On the other hand, energy and strength of resonances are difficult to predict with the required accuracy. The situation is somewhat improved whenever the statistical model of nuclear reactions (Hauser-Feshbach theory) can be applied, which uses resonance averages. Fortunately, the majority of reactions in astrophysics involving the strong interaction can be described in this approach [61]. When predicting cross sections for astrophysical applications in such a way, slightly different points are emphasized than in pure nuclear physics investigations. Since most of the ingredients for the calculations are experimentally undetermined (in some cases even for nuclides at or close to stability), one has to develop reliable phenomenological or microscopic models to predict these properties with an acceptable accuracy across the nuclear chart. Therein one has to be satisfied with a more limited accuracy as compared to usual nuclear physics standards. Considering the substantially larger uncertainties in many astrophysical scenarios, this seems to be adequate. For certain selected reactions, however, the sensitivity of the astrophysical results is so high that an accuracy of 10% or better is necessary. Examples of this are the reactions ^{12}C(α,γ)^{16}O and (α,n) and (α,γ) on ^{22}Ne, as discussed below. When studying details in s-process branchings, cross sections have to be determined to 1%. This is currently only possible with experiments or by a combination of experiment and theory, e.g. when supplementing resonance measurements with direct capture calculations.

In this review I first present new calculations of the evolution and nucleosynthesis of massive stars, involving reaction networks of unprecedented size. A non-exhaustive selection of important nuclear reactions is then given and their importance is shown by the impact on the results. In the second part of the paper, the current standard approach to predict nuclear cross sections and reaction rates is outlined and the remaining uncertainties and challenges are illustrated by a few examples.

2. Nucleosynthesis in massive stars

2.1. The model

Stars above $\sim$ 10 $M_\odot$ are responsible for producing most of the oxygen and heavier elements found in nature. Numerous studies have been devoted to the evolution of such stars and their nucleosynthetic yields. However, our knowledge of both the input data and the physical processes affecting the evolution of these stars has improved dramatically in recent years. Thus, it became worthwhile to improve on and considerably extend the previous investigations of pre– and post–collapse evolution and nucleosynthesis. The first calculation to determine, self-consistently, the complete synthesis of all stable nuclides in any model for a massive star [56] is discussed here. The calculations were performed using the stellar evolution code KEPLER [76] with several modifications relative to [76] (mass loss due to stellar winds, improved adaptive network) and updates (OPAL95 opacity tables, neutrino loss rates). According to the topic of this report, the focus is on giving an outline of the updates concerning the nuclear reactions involving the strong interaction. For further details of the calculations and results the reader is referred to the full paper [56].

As in [76], two reaction networks are used. A small network directly coupled to the

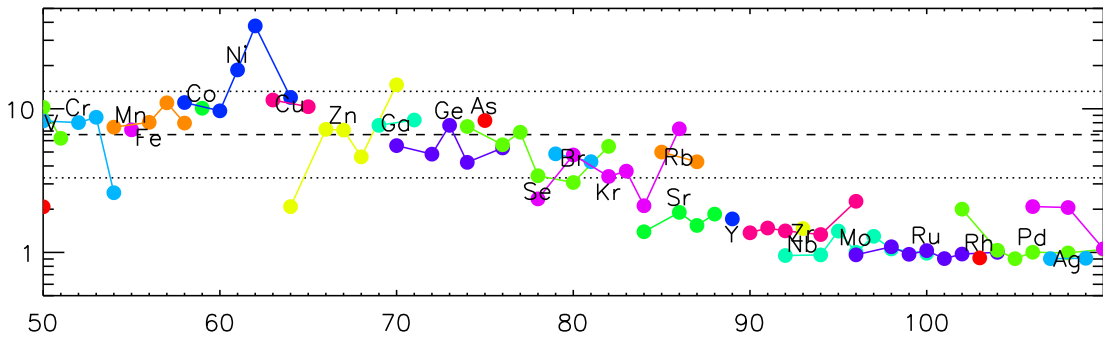

Figure 1. Postexplosive production factors (vertical axis) versus mass number (horizontal axis) of a population I star with 15 $M_\odot$ progenitor mass. The horizontal axis Comparison is relative to solar abundances. The relative overproduction of ^{61,62}Ni may indicate some inherent nuclear uncertainty in the (n,γ) destruction cross section. See text and the full paper [56] for details.

stellar model calculation provides nuclear energy generation, i.e. it is solved implicitly for each time-step in each zone. This smaller network is essentially the same as in [76], but with updated nuclear rates as described in the following.

One of the major improvements over [76] and other stellar models is that, for the first time, the synthesis of all nuclides of any appreciable abundance is followed simultaneously in an *adaptive network* of unprecedented size. Using a library containing rate information for 4,679 isotopes from hydrogen to astatine, the "adaptive" network automatically adjusts its size to accommodate the current nuclear flows. This saves CPU time and thus allows to perform the calculations within reasonable time. Because of convective coupling of zones, the same network must be used throughout the star.

Within such a network, the impact of nuclear rates on burning and evolution of the star can be studied fully self-consistently.

2.2. Nuclear input

The most extensive published library of theoretical reaction rates to date [59,60] was used as the backbone of the reaction rate sets. Details of the predictions are given in Sec. 3. For the network described here, the rates based on the FRDM set were implemented. This theoretical set was supplemented with experimental neutron capture rates along the line of stability [5]. Experimental (α,γ) rates were implemented for ^{70}Ge [18] and ^{144}Sm [67]. The derived α+^{70}Ge and α+^{144}Sm potentials were also utilized to recalculate the transfer reactions involving these potentials. Semi-empirical rates were implemented for α-capture reactions on self-conjugated ($N = Z$) nuclides [63]. For the important rate ^{12}C(α,γ)^{16}O we used an updated rate ($S(300) = 146$ keV barn $= 1.2\times$ Ref. [10]) and temperature dependence [10]. Similarly important is the (α,n)/(α,γ) branching [34] on ^{22}Ne (see [75]). Table 1 defines the standard rate set. For comparison, additional sets of experimental and theoretical rates were used for elements below neon: Refs. [76,28] and NACRE [3]. Experimental β^-, β^+, and α-decay rates were taken from [70] and theoretical

Table 1
Nuclear reaction rate inputs (for details see Tables 1 and 2 in Ref. [56]).

Reference	Type
Bao et al. (2000) [5]	(n,γ)
Buchmann (1996) [10]	^{12}C(α,γ), modified (see Woosley, this volume)
Caughlan & Fowler (1988) [12]	light targets, charged projectiles
Fowler, Caughlan & Zimmerman (1975) [17]	light targets, charged projectiles
Fülöp et al. (1996) [18]	^{70}Ge(α,γ)
Giessen et al. (1994) [20]	^{18}O(α,γ)
Harris et al. (1983) [24]	light targets, charged projectiles
Hansper et al. (1989) [23]	^{45}Sc(α,p), ^{45}Sc(α,n)
Iliadis et al. (2001) [31]	(p,γ)
Käppeler et al. (1994) [34]	^{22}Ne+α, modified (see Woosley, this volume)
Kiener et al. (1993) [35]	^{13}N(p,γ)
Landré et al. (1990) [39]	^{14}N(α,p), ^{17}O(p,γ)
Mitchell et al. (1985) [43]	^{42}Ca+α
Morton et al. (1992) [50]	^{48}Ti(α,p)
Rauscher & Thielemann (2000,2001) [59,60]	theory
Rauscher et al. (1994) [62]	light targets, neutron- and α-induced
Rauscher et al. (2000) [63]	α-capture on isospin symmetric targets
Somorjai et al. (1998) [67]	^{144}Sm(α,γ)
Scott et al. (1992) [65]	^{34}S+α
Sevior et al. (1986) [66]	^{38}Ar+α
Scott et al. (1991) [64]	^{41}K(α,p)
Wrean et al. (1994) [77]	^{9}Be(α,n)
Wiescher & Kettner (1982) [73]	^{15}O(α,p)
Winters & Macklin (1988) [74]	^{20}Ne(n,γ)

β^- and β^+ rates from [48]. As a special case, a temperature-dependent ^{180}Ta decay [6] was implemented. The production ratio ^{180m}Ta/^{180}Ta had to be computed offline (after production and ejection) because the isomer was not included in the network as a separate species. The estimate of this ratio is based on the data of [6] and a derivation given in Appendix B of [56].

For $A \leq 40$ recent theoretical weak rates [41] were also included. The ν-process was not followed for nuclides with Z or N larger than 40 and neither was a possible r-process in high-entropy layers close to the surface of the proto-neutron star. However, a slight n-process could be found, due to high neutron flux generated at the base of the He-shell [56].

2.3. A non-exhaustive selection of important reactions

It should be noted that only a selection of a few important rates is presented in this section. If a reaction does not show up here, this does not imply that it is of no importance. It just means that there was not sufficient space to discuss the reaction properly. Main reactions in the quiescent burning phases of a star (e.g. ^{12}C+^{12}C in carbon burning) as well as those many neutron capture reactions necessary for a detailed study of s-process branchings will always remain on the list of important reactions. However, a few reactions were chosen subjectively for discussion here.

2.3.1. ^{12}C(α,γ)^{16}O

It is well known that the leading nuclear uncertainty afflicting modern studies of stellar evolution and nucleosynthesis continues to be the reaction rate of ^{12}C(α,γ)^{16}O. This reaction competes for the consumption of α-particles with the triple-alpha reaction during helium burning. It determines the ratio of C to O at the onset of the subsequent burning stage, i.e. carbon burning. This has important implications not only for nucleosynthesis but determines the further evolution of the star and even the nature of the collapse and explosion.

Weaver & Woosley [72] suggested a preferred value of 170±20 keV b for the total S-factor at 300 keV, based on nucleosynthesis arguments. Recently, those calculations were repeated using more modern stellar models [26] and arrived at basically the same conclusions as [72]. For that reason, the currently preferred choice for the absolute value and energy dependence of the rate is the one given in Sec. 2.2.

A further implication of the nucleosynthesis study is that the rate has to be known to an accuracy of $\leq 10\%$. Recent measurements [10,11,9,38,69] give recommended values in the range 145 to 165 keV b but with considerable uncertainty. Only the work of Tischhauser *et al.* [69] is beginning to approach that precision.

2.3.2. ^{22}Ne(α,γ)^{26}Mg and ^{22}Ne(α,n)^{25}Mg

Behind ^{12}C(α,γ)^{16}O, the ^{22}Ne(α,n) rate and the (α,n)/(α,γ) branching at ^{22}Ne become the second largest nuclear uncertainties in calculating the nucleosynthesis in massive stars. The weak s-process component, including a large number of nuclides produced by neutron captures up to about $A = 90$, is made in massive stars. The relative production of these nuclei compared to other abundant species like O and to one another is sensitive to the cross sections of neutron poisons like ^{25}Mg and ^{16}O [75], and to the rate of ^{22}Ne(α,n)^{25}Mg.

The (α,n) rate has always been quite uncertain [3]. Recent experimental work [32] exhibits higher accuracy but is still uncertain enough to accommodate a factor of two uncertainty in many important s-process products for $80 \leq A \leq 90$ (see Fig. 2).

2.3.3. The ^{62}Ni(n,γ) case

This case is a good example of the difficulties encountered when trying to predict reaction rates for final nuclei with low level densities. For neutron-induced reactions at low energies, close to magic numbers, and far off stability where low separation energies are encountered, a problem emerges. In such targets, the level density is too low to allow the application of the statistical model [61]. Also for other nuclides it is not straightforward to bridge the region of thermal energies to the region of overlapping resonances where the Hauser-Feshbach formalism can be used. Single resonances and direct reactions become important. This is also an issue for neutron-rich nuclei in the r-process path with low neutron-separation energies.

With the reaction ^{62}Ni(n,γ)^{63}Ni it was previously attempted to extrapolate thermal data to s-process energies of up to a few hundred keV. Two compilations give disagreeing 30 keV cross sections [4,5], based on the same thermal data. Both extrapolations assume s-wave behavior of a direct capture component. The more recent one includes a subthreshold resonance contributing to the thermal cross section.

A calculation of the direct capture component using DWBA found a considerable p-wave contribution which enhances the cross section at 30 keV [57]. Thus, even when

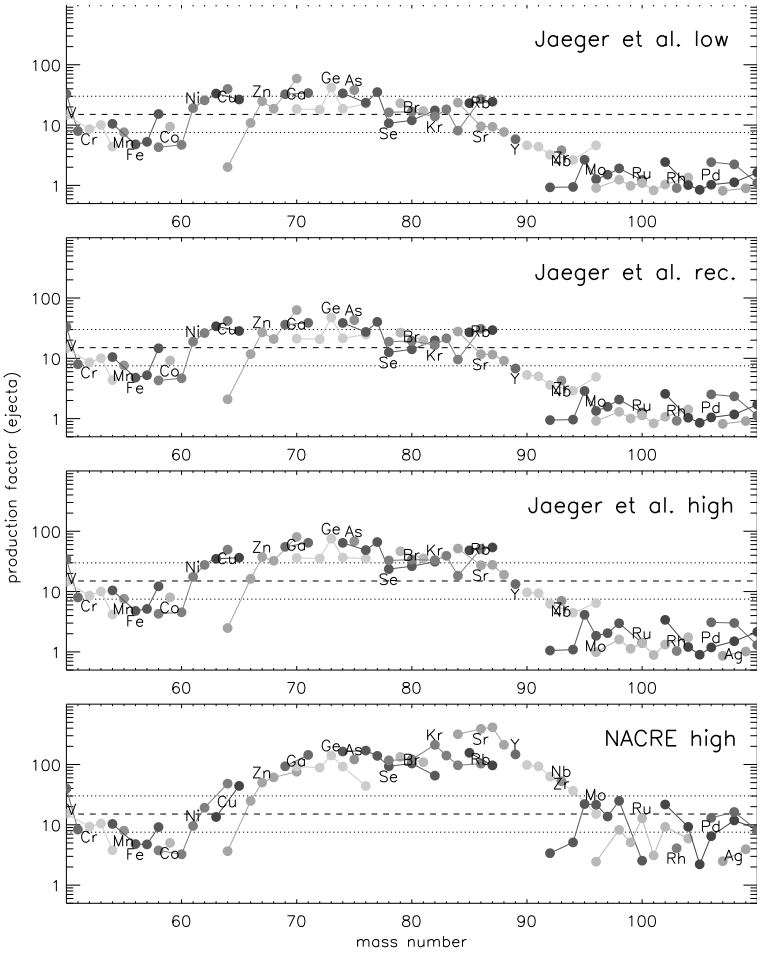

Figure 2. Nucleosynthesis of the weak s-process with varied rate of ^{22}Ne(α,n)^{25}Mg in a 25 $M_\odot$ star of initial solar metallicity. A factor of two overproduction (dotted lines) is acceptable because lower mass stars make less s-process and low metallicity stars make very little.

including the subthreshold resonance, the 30 keV value is coincidentally similar to the value in the older compilation (Fig. 3). However, also the general energy dependence of the cross section is altered. Resonances were also included but they only contribute less than 15%. The enhanced cross section has an important impact on *s*-processing in massive stars. The previously seen overproduction of ^{62}Ni in stellar models (see Fig. 1) can be cured when using the enhanced rate because of increased destruction of this nucleus with the larger neutron capture rate [56,57]. An experimental verification of this result would be desireable.

Further neutron capture reactions on Ni isotopes might also be suspect but they do not show the additional complication of a sub-threshold resonance.

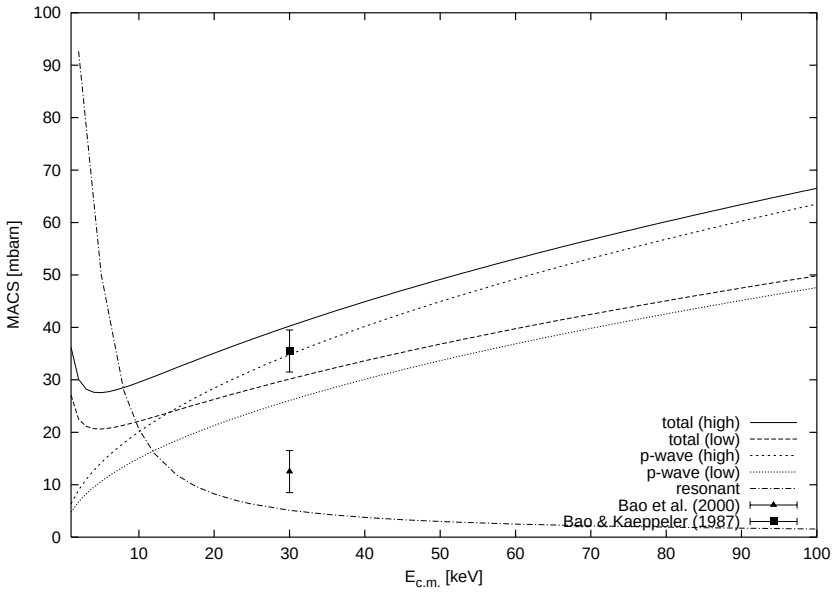

Figure 3. Direct neutron capture Maxwellian averaged cross section of ^{62}Ni. The final value is given by adding the resonant contribution to the "total" direct term. Upper and lower limits on the direct components are from experimental errors on the input, *i.e.* in the thermal scattering length and the spectroscopic factors.

3. Statistical model calculations

3.1. A reaction rate library

A recently published large-scale reaction rate library includes neutron-, proton-, and α-induced reactions on all target nuclei from Ne up to Bi from proton-dripline to neutron-dripline [59,60]. Due to the fact that many very short-lived nuclides can be produced in astrophysical sites, it is necessary to provide cross sections and rates for about 4600 targets and 32000 reactions. These numbers show that theory will always play a major role in providing cross sections, despite the potential of future Rare Isotope Accelerators. This rate library has already been adopted as a standard for calculating nucleosynthesis in stellar evolution and in type II supernovae [56,25]. Fits to the astrophysical reaction rates – ready for direct astrophysical application – as well as tables of cross sections, reaction rates, and nuclear inputs for all possible reactions with light projectiles can also be downloaded from *http://nucastro.org/reaclib.html* .

3.2. Global calculations

The calculations for the above library were performed with the Hauser-Feshbach code NON-SMOKER [58] which is especially tuned to such large-scale predictions. The theoretical determination of nuclear properties in this code is based on microscopic or macroscopic-microscopic approaches suitable for an application far off stability. As mentioned before, due to the large number of unstable nuclei to be implemented in nuclear reaction networks for astrophysics, nuclear properties needed for the calculation of reaction rates have to

be predicted. Necessarily, there is a trade-off with accuracy because one cannot expect to predict those properties with similar accuracy as measured data. However, whenever measured properties can be used, this will, of course, lead to an improvement in the calculated rates. Unfortunately, this is not possible for the vast majority of reactions off the line of stability (and sometimes not even at stability).

Occasionally, a misconception about the best models for nuclear properties seems to arise. The question is not merely one of microscopic versus phenomenological approaches, it should rather be "*what can we learn from the different models and how do we implement the findings in a simple way, suited for large-scale computations?*". On one hand, first-principles microscopic models can be more satisfying from a philosophical point of view. Such a model will of course be most preferrable as soon as the perfect one has been identified. Unfortunately, the current state-of-art sees competition of many different microscopic approaches, each with its own advantages and drawbacks, but we are still far from a complete, unified picture. Thus, one has to be careful when using the term "microscopic" in the sense of a general remedy.

On the other hand, the problem inherent in all microscopic approches is that they are CPU expensive. Although further progress regarding CPU speed and perhaps algorithmical effectiveness can be expected, this will hamper large-scale studies for some time to come. A more effective approach is to *understand* the important effects found in microscopic calculations or based on *fundamental properties* of nuclei and to derive a simple, even if phenomenological or parametrized, way to implement them in the reaction rate calculations. A good example for using microscopic (in this case, shell model Monte Carlo) calculations in this way is the treatment of the parity distribution in nuclei at low excitation energies, as discussed in Sec. 3.3.2. An example of using fundamental properties of nuclei is the approach to calculate nuclear level densities (Sec. 3.3.1).

In the NON-SMOKER code it was tried to implement reliable predictions of nuclear properties following the above philosophy. For instance, the nucleon optical potentials are calculated in a fast microscopic model [33]. The photon transmission coefficients are derived using a global parametrization of GDR properties [68], based on the hydrodynamic droplet model and including an energy-dependent GDR width [59]. Further included are width fluctuation corrections and isospin effects [58]. The nuclear level density will be discussed in the following section. Details of all nuclear properties used are given elsewhere [59,58].

3.3. Nuclear Level Density

3.3.1. A global description

The nuclear level density is an important ingredient in the prediction of nuclear reaction rates in astrophysics. The applicability of the statistical model of nuclear reactions (Hauser-Feshbach formalism) can be derived from the average level spacing and lower limits of energy and temperature for the application to calculate cross sections and reaction rates, respectively, can be given [61].

The current version of the NON-SMOKER code uses a level density description based on *fundamental properties* of nuclei, as introduced above. The macroscopic properties can be derived from the Fermi-gas formalism [8]. Obviously, these will hold as long as the nucleons can be described by a Fermi-gas, regardless of whether they are close to or far

from stability. Pairing is usually accounted for by introducing a backshift, leading to the well-known expressions of the shifted Fermi-gas [7]:

$$\rho(U,J,\pi) = \mathcal{F}(U,J,\pi)\rho(U) \quad , \tag{1}$$

with

$$\rho(U) \propto \frac{1}{\sigma a^{1/4}} \frac{\exp(2\sqrt{aU})}{U^{5/4}} \tag{2}$$

$$\sigma^2 = \frac{\Theta_{\rm rigid}}{\hbar^2}\sqrt{\frac{U}{a}} \ , \qquad U = E - \delta \quad .$$

The spin and parity dependence $\mathcal{F}$ is determined by the spin cut-off parameter σ. Thus, the level density is dependent on only two parameters: the level density parameter a and the backshift δ, which determines the energy of the first excited state. The divergence for $E = \delta$ can be avoided by either introducing an additional term depending on the nuclear temperature [40] or by matching it to the constant temperature formula at low energies [61].

Within this framework, the quality of level density predictions depends on the reliability of systematic estimates of a and δ. All current (microscopic) calculations prove that the backshifted Fermi-gas can account for the nuclear level density as long as a and δ are chosen properly, e.g. Shell Model Monte Carlo [2,13], combinatorial approaches [52], and recurrence relations for exact level densities [71].

Thus, while the overall shape of the energy dependence is given by the globally valid Fermi-gas, the microscopic corrections enter via δ and mainly via a:

$$a(U,Z,N) = \tilde{a}(A)\left[1 + C(Z,N)\frac{f(U)}{U}\right] \quad , \tag{3}$$

where

$$\tilde{a}(A) = \alpha A + \beta A^{2/3} \tag{4}$$

and

$$f(U) = 1 - \exp(-\gamma U) \quad . \tag{5}$$

Therefore, the parameter a contains all effects *beyond* a spherical droplet. Here, the microscopic correction $C(Z,N)$ is thermally damped away at high excitation energies as suggested by [29,30] after inspection of hydrodynamic models. Three free parameters α, β, γ have to be fitted to nuclear data. The strength of the above approach lies in the fact that these *microscopic properties* can easily be extracted from other (microscopic or semi-microscopic) calculations which are available across the whole nuclear chart: nuclear mass models. Many different inputs can easily be implemented and compared. This is explained in detail in [61].

Obviously, the resulting level density inherits the deficiencies of the underlying model concerning the microscopic properties. This is illustrated by Fig. 4 for two cases. Nevertheless, for the majority of nuclei deviations of less than a factor of two can be obtained

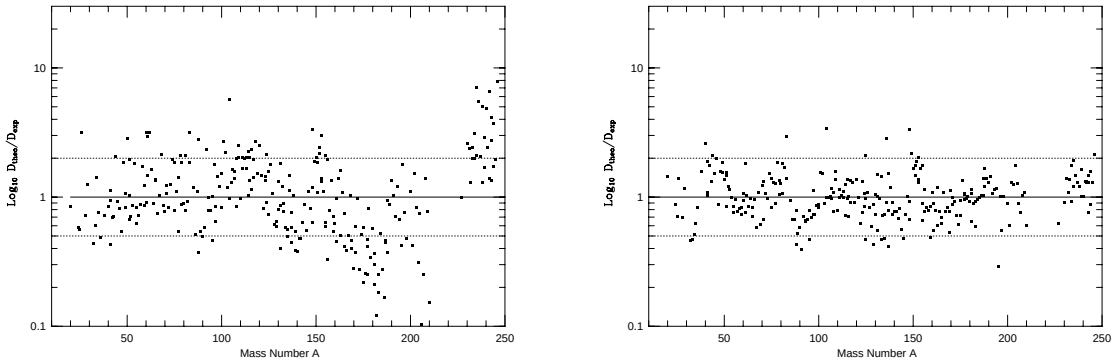

Figure 4. Ratio of predicted to experimental level densities at the neutron separation energy with microscopic inputs taken from [27] (left) and from [49] (right). The deficiencies of the underlying mass formula are propagated to the level density result. For instance, the well-known problems of [27] at higher mass numbers can be seen clearly. Using input from [49] improves the situation drastically. However, shell closures are still overpronounced as can be seen from the emerging pattern in the level density ratios.

when using, for instance the FRDM input [49], which translates into a much lower uncertainty (about 30%) in the reaction rates. It has to be emphasized that the accuracy of this purely theoretical approach is still unsurpassed, despite recent attempts for improvement with other approaches, e.g. [22,14] (it should be noted that the average deviation quoted in [14] includes results which were renormalized to experiment and therefore is not a measure of predictive power).

For all details of the level density description and further implications, please refer to the extended paper [61].

3.3.2. Implementing parity-dependence

So far, all theoretical, global calculations of astrophysical rates assume an equal distribution of the state parities at all energies. It is obvious that this assumption is not valid at low excitation energies of a nucleus. However, a globally applicable recipe was lacking. We combine a formula for the energy-dependent parity distribution [1] with the microscopic-macroscopic nuclear level density described above [45,44]. The formula reproduces well the transition from low excitation energies where a single parity dominates to high excitations where the two densities are equal. It was tested against Monte Carlo shell model calculations.

Alhassid *et al.* [1] have introduced a simple model for the partition function ratio Z_-/Z_+ for nuclei in the iron region using the complete $pf + g_{9/2}$ shell. This model was combined with the shifted Fermi-gas approach to derive parity-dependent level densities. For details, see [45,44].

The parity-dependent level density was used to calculate astrophysical reaction rates

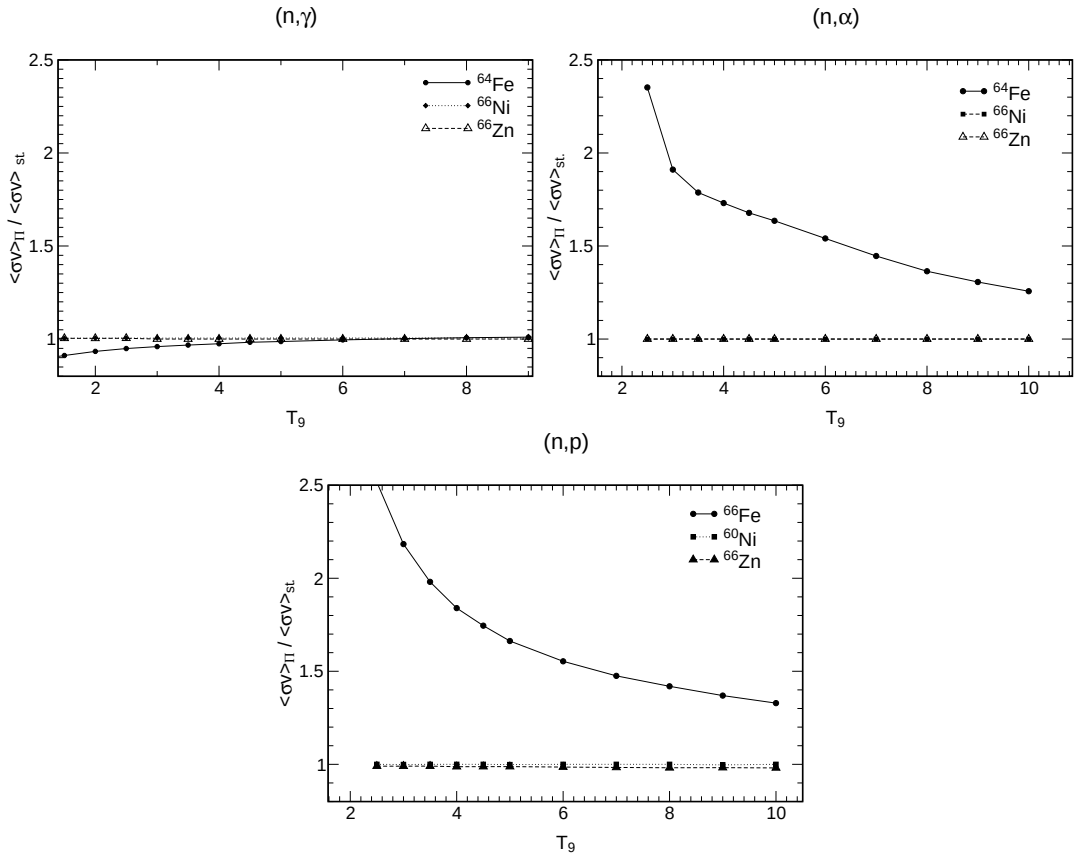

Figure 5. Comparison of the parity dependent reaction rates to the standard [60], which assumes an equal distribution of odd and even parity states. The *final* nucleus is specified for each reaction.

involving the three nuclides ^{64}Fe, ^{66}Ni, ^{68}Zn in the global Hauser-Feshbach model NON-SMOKER. A comparison to the standard values is shown in Fig. 5. The impact on the rates involving the Ni and Zn nuclei is small and negligible compared to the remaining uncertainties in the global HF model. This is due to the fact that a sufficiently large number of excited states is known experimentally. Up to 20 experimental states are considered in the standard calculation and only above the last known state, the theoretical level density is in effect. However, the case is different for reactions involving ^{64}Fe. No information on experimental states is known here and therefore the full impact of the parity dependence can be seen. In the (n,γ) case 20% difference are found. Much larger differences are seen in the reactions involving ^{64}Fe in the final particle channel. Because of lack of negative parities at low excitation energies, the particle emission channel becomes strongly enhanced in all such reactions with low or negative Q values. The (n,γ) channel show lower sensitivity because the total transmission coefficient includes more transitions to states at higher excitation energy where the parity ratio is already close to unity. This is not true for the particle (exit) channels where preferrably states at low excitation energy

are populated, due to the reaction energetics.

The case for ^{64}Fe shows that a large effect of the parity dependence can be expected far from stability where no experimental information on excited states is available and that it is extremely important to include such a modified level density. The current approach is valid only for even-even nuclei in the $pf + g_{9/2}$ shell. Work is in progress to extend this description to be able to calculate the parity distribution for a large number of nuclei far from stability on the proton-rich as well as neutron-rich side.

3.4. Optical α-nucleus potentials

There have only been few attempts to derive global optical potentials for α-projectiles [54] and most of them are only valid at α-energies larger than 30 MeV. Due to the high Coulomb barrier and nuclear structure effects defining the imaginary part of the potential it is difficult to obtain a global potential at astrophysical energies. Elastic α-scattering data can constrain the real part of the potential [42,47] and detailed analysis can also improve on the imaginary part [46,19], describing the absorption into other channels than the elastic scattering, i.e. the Hauser-Feshbach channel. Due to the scarcity of data for intermediate and heavy nuclei, attempts to improve on the potential are mostly concentrating on single reactions [67,19]. More global approaches suffer from the lack of data to confine their parameters [54,15].

Recently, it was tried [16] to find a potential for the $A \simeq 140$ mass region by simultaneously fitting data for ^{143}Nd(n,α)^{140}Ce [36], ^{147}Sm(n,α)^{144}Nd [21], and ^{144}Sm(α,γ)^{148}Gd [67]. The optical potential is parametrized as

$$V(r,E) = -\frac{V_0}{1+\exp\left(\frac{r-r_r A^{1/3}}{a_r}\right)} - i\frac{W(E)}{1+\exp\left(\frac{r-r_V A^{1/3}}{a_V}\right)} \quad . \tag{6}$$

Different parameters for the potential geometry and the energy dependence of the depth of the imaginary part were explored [16,55]. No significant differences were found between using a Brown-Rho shape [47] $W(E) = W_0((E-E_0)^2)/((E-E_0)^2+\Delta^2)$ or a Fermi-type shape [67] $W(E) = W_0/(1+\exp((E^*-E)/a^*))$ of the energy dependence. For the latter, the parameters $E^* = 18.74$ MeV, $a^* = 2.1$ MeV were found, with all other parameters as in the previous paper [67]. The Brown-Rho best fit was obtained with $E_0 = 6.35$ MeV and $\Delta = 28.4$ MeV, with the same fixed parameters $V_0 = 162$ MeV, $r_r = 1.27$ fm, $a_r = 0.48$ fm, $W_0 = 19$ MeV, $r_V = 1.57$ fm, $a_V = 0.6$ fm. The results from the simultaneous fit of three reactions are shown in Figs. 6 and 7.

Despite the fact that the considered targets are in the same mass region, the derived parameters also describe acceptably well the reaction ^{96}Ru(α,γ)^{100}Pd [53]. However, it is remarkable that even better overall agreement with all four reactions can be obtained when using a mass- and energy-independent potential of Saxon-Woods form for the real and imaginary parts (see Fig. 8). The real parameters are given by $V_0 = 162.3$ MeV, $r_r = 1.27$ fm, $a_r = 0.48$ fm, the imaginary ones by $W_0(E) = W_V = 25$ MeV, $r_V = 1.4$ fm, $a_V = 0.52$ fm. Thus, the real part is identical to the potential by Somorjai *et al.* [67] but without energy dependence, whereas the imaginary part is similar to the one used in McFadden & Satchler [67]. Since the McFadden & Satchler parameters were derived from extensive elastic scattering data it seems reasonable that they are applicable to a wider range of targets. The Somorjai *et al.* parameters were derived for one reaction only

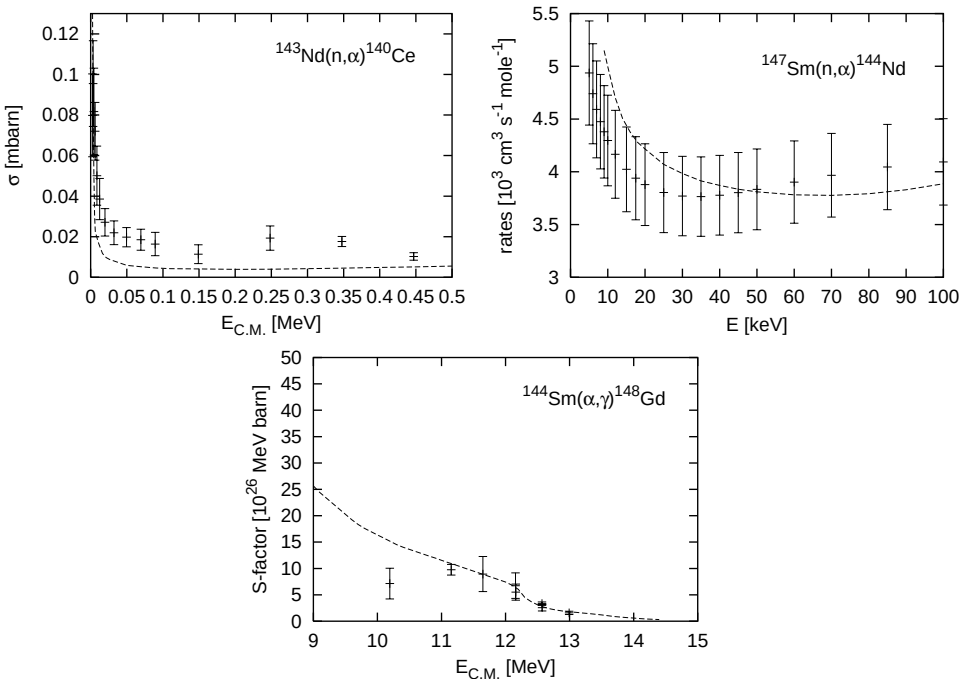

Figure 6. Cross sections, reaction rates, and S-factors from a simultaneous χ^2 fit of the Fermi-type energy-dependent α+nucleus optical potentials of three reactions (see text). The dashed lines are the statistical model calculation. The errors on the ^{147}Sm(n,α) rates were assumed to be 10%.

but seem to work also for the nuclides investigated here. The new energy-independent potential also describes well other reactions not shown here, e.g. ^{70}Ge(α,γ)^{74}Se.

Here, we do not show our results from fitting each reaction separately. Obviously, potentials fitted to single reactions can describe those – but only those – even better.

Closer examination of Fig. 8 seems to suggest that an additional energy-dependence has to be introduced at very low α-energies. This can be seen mainly from the ^{144}Sm(α,γ) comparison. However, since so far comparisons to other reactions were successful and the potentials only failed for this one case, it could also be that this is just a peculiar reaction. One peculiarity is the α-decay of the final nucleus ^{148}Gd. In fact, in the considered reactions, also ^{144}Nd is an α-emitter. As can also be seen from Figs. 6–8, the description of ^{147}Sm(α,n)^{144}Nd is always less good than of those reactions without α-unstable final nucleus. This is supported by the fact that non-statistical effects have been found in this reaction [37]. It seems that an additional effect has to be included for α-unstable nuclides, either by a modified phenomenological potential or by explicitly accounting for the correction. In the case of ^{144}Sm(α,γ), the effect seems to start acting at around 12 MeV, perhaps similar to an additional barrier.

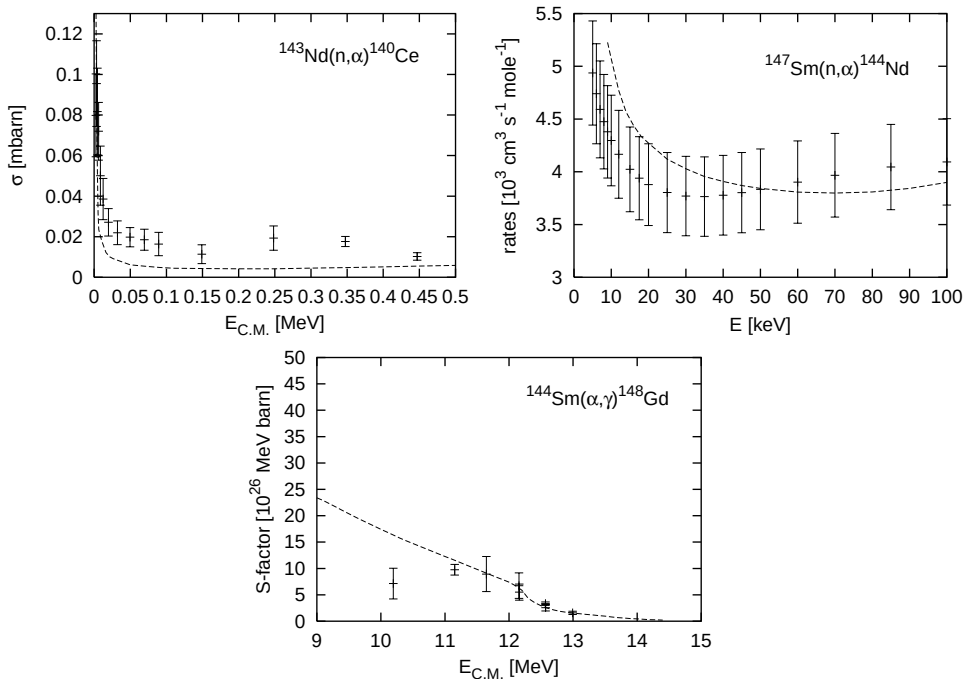

Figure 7. Cross sections, reaction rates, and S-factors from a simultaneous χ^2 fit of the Brown-Rho energy-dependent α+nucleus optical potentials of three reactions (see text). The dashed lines are the statistical model calculation. The errors on the ^{147}Sm(n,α) rates were assumed to be 10%.

4. Conclusions

Stellar models have now reached a stage where the often quoted astrophysical accuracy of "a factor of two" is not sufficient anymore in many cases. This poses a special challenge for the experimentalist as well as the theoretician. Global nuclear models have already been quite successful in predicting nuclear rates, especially for neutron- and proton-induced reactions. Despite these considerable successes close to and far off stability, the description of certain nuclear inputs, such as optical α-potentials, still needs to be improved. It is also still unclear whether nuclear properties far off stability can be predicted with sufficiently high accuracy. Although future advances in microscopic theories may alleviate that problem, experimental data is clearly needed. Rare Isotope Accelerators will make it possible to study highly unstable nuclides but also "classical" nuclear physics experiments with stable or long-lived nuclei are indispensable. They are not only required to study specific crucial reactions in stellar evolution and nucleosynthesis but can also provide the systematics for global descriptions and shed light on the interaction of different reaction mechanisms.

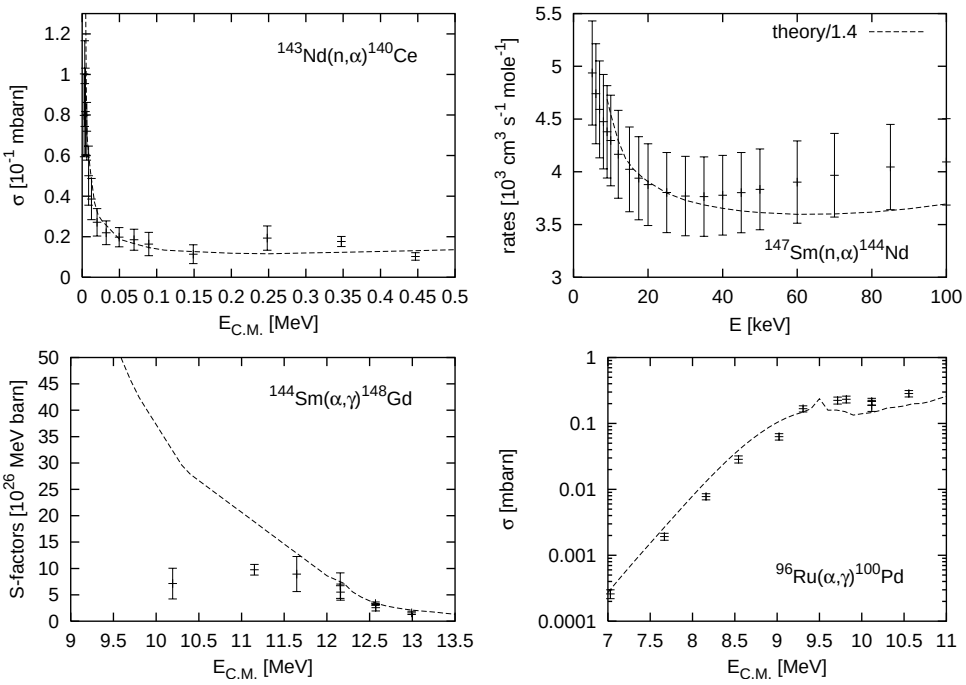

Figure 8. Results for four different reactions using the new energy-independent potential from [16,55] (see text). The dashed lines are the statistical model calculation. Note that the ^{147}Sm(n,α) result is renormalized by a factor 1/1.4.

Acknowledgements

I thank my collaborators Y. Alhassid, C. Fröhlich, A. Heger, R. D. Hoffman, G. Martinez-Pinedo, F.-K. Thielemann, and S. E. Woosley. This work was supported in part by the Swiss NSF grants 2000-061031.02, 2024-067428.01. I am also grateful for having received a PROFIL professorship from the Swiss NSF.

REFERENCES

1. Y. Alhassid, G. F. Bertsch, S. Liu and H. Nakada, Phys. Rev. Lett. 84 (2000) 4313.
2. Y. Alhassid, S. Liu, and H. Nakada, Phys. Rev. Lett. 83 (1999) 4265.
3. C. Angulo, et al., Nucl. Phys. A656 (1999) 3.
4. Z.Y. Bao and F. Käppeler, ADNDT 36 (1987) 411.
5. Z. Bao, et al., ADNDT 76 (2000) 1.
6. D. Belic, et al., Phys. Rev. Lett. 83 (1999) 5242.
7. A. H. Bethe, Phys. Rev. 50 (1936) 332.
8. A. Bohr and B. R. Mottelson, *Nuclear Structure* (World Scientific, 1998).
9. C. R. Brune, Phys. Rev. C 64 (2001) 055803.
10. L. Buchmann, Astrophys. J. 468 (1996) L127; L. Buchmann, priv. comm. (2000).
11. L. Buchmann, Astrophys. J. 479 (1997) L153.
12. G.A. Caughlan and W.A. Fowler, ADNDT 40 (1988) 283.
13. D. Dean, et al., Phys. Rev. Lett. 74 (1995) 2909.
14. P. Demetriou and S. Goriely, Nucl. Phys. A695 (2001) 95.
15. P. Demetriou, C. Grama, and S. Goriely, Nucl. Phys. A707 (2002) 253.
16. C. Fröhlich, diploma thesis, University of Basel, unpublished (2002).
17. W.A. Fowler, G.R. Caughlan, and B.A. Zimmerman, Ann. Rev. Astron. Astrophys. 13 (1975) 69
18. Zs. Fülöp, et al., Z. Phys. A 355 (1996) 203.

19. Zs. Fülöp et al., Phys. Rev. C 64 (2001) 065805.
20. U. Giessen, et al., Nucl. Phys. A567 (1994) 146.
21. Yu.M. Gledenov, P.E. Koehler, J. Andrzejewski, K.H. Guber and T. Rauscher, Phys. Rev. C 62 (2001) 042801(R).
22. S. Goriely, Nucl. Phys. A605 (1996) 28.
23. V. Hansper, et al., Univ. of Melborne School of Physics preprint UM-P-89/30 (1989).
24. M.J. Harris, et al., Ann. Rev. Astron. Astrophys. 21 (1983) 165.
25. A. Heger, T. Rauscher, R. D. Hoffman, and S. E. Woosley, Nucl. Phys. A, in press (2002).
26. A. Heger, S. E. Woosley, and M. Boyes, Astrophys. J., in preparation (2002); see also M. Boyes, UCSC Sr. Thesis, 2002.
27. E. R. Hilf, H. von Groote, and K. Takahashi, in *Proc. 3rd Int. Conf. Nuclei far from Stability*, CERN report 76-13 (1976), p. 142.
28. R.D. Hoffman, S.E. Woosley, and T.A. Weaver, Astrophys. J. 594 (2001) 1085.
29. A. V. Ignatyuk, G. N. Smirenkin, and A. S. Tishin, Yad. Fiz. 21 (1975) 485.
30. A. V. Ignatyuk, K. K. Istekov, and G. N. Smirenkin, Sov. J. Nucl. Phys. 29 (1979) 450.
31. C.A. Iliadis, et al., Astrophys. J. Suppl. 134 (2001) 151.
32. M. Jaeger, et al., Phys. Rev. Lett. 87 (2001) 202501.
33. J. P. Jeukenne, A. Lejeune, and C. Mahaux, Phys. Rev. C 16 (1977) 80.
34. F. Käppeler, et al., Astrophys. J. 437 (1994) 396.
35. J. Kiener, et al., Nucl. Phys. A552 (1993) 66.
36. P. E. Koehler, priv. comm. (2001).
37. P. E. Koehler, Yu. M. Gledenov, and T. Rauscher, Phys. Rev. C, in preparation (2002).
38. R. Kunz, et al., Astrophys. J. 567 (2002) 643.
39. V. Landré, et al., Astron. Astrophys. 240 (1990) 85.
40. J. M. B. Lang and K. J. LeCouteur, Proc. Phys. Soc. London A 67 (1954) 585.
41. K. Langanke and G. Martínez-Pinedo, Nucl. Phys. A673 (2000) 481.
42. L. McFadden and G. R. Satchler, Nucl. Phys. 84 (1965) 177.
43. L. Mitchell, et al., Univ. of Melborne School of Physics preprint UM-P-85/11 (1985).
44. D. Mocelj, T. Rauscher, G. Martinez-Pinedo, and Y. Alhassid, in *Proc. CGS 11* (World Scientific, 2003), in press.
45. D. Mocelj, T. Rauscher, G. Martinez-Pinedo, and Y. Alhassid, Nucl. Phys. A, in press (2002).
46. P. Mohr, Phys. Rev. C 61 (2000) 045802.
47. P. Mohr, et al., Phys. Rev. C 55 (1997) 1523.
48. P. Möller, J.R. Nix, and K.L. Kratz, ADNDT 66 (1997) 131.
49. P. Möller, J.R. Nix, W. D. Myers, and W. J. Swiatecki, ADNDT 59 (1995) 185.
50. A.J. Morton, et al., Nucl. Phys. A537 (1992) 167.
51. H. Nakada and Y. Alhassid, Phys. Lett. B79 (1998) 231.
52. V. Paar and R. Pezer, Phys. Rev. C 55 (1997) R1637.
53. W. Rapp et al., Phys. Rev. C 66 (2002) 015803.
54. T. Rauscher, in *Nuclei in the Cosmos IV*, eds. N. Prantzos, S. Harissopulos (Editions Frontières, Gif-sur-Yvette 1998), p. 484.
55. T. Rauscher, C. Fröhlich, and K. Guber, in *Proc. CGS 11* (World Scientific, 2003), in press.
56. T. Rauscher, A. Heger, R.D. Hoffman and S.E. Woosley, Astrophys. J. 576 (2002) 323.
57. T. Rauscher and K.H. Guber, Phys. Rev. C 66 (2002) 028802.
58. T. Rauscher and F.-K. Thielemann, in *Stellar Evolution, Stellar Explosions, and Galactic Chemical Evolution*, ed. A. Mezzacappa (IOP, Bristol 1998), p. 519.
59. T. Rauscher and F.-K. Thielemann, ADNDT 75 (2000) 1.
60. T. Rauscher and F.-K. Thielemann, ADNDT 79 (2001) 47.
61. T. Rauscher, F.-K. Thielemann and K.-L. Kratz, Phys. Rev. C 56 (1997) 1613.
62. T. Rauscher, et al., Astrophys. J. 429 (1994) 499.
63. T. Rauscher, et al., Nucl. Phys. A675 (2000) 695.
64. A.F. Scott, et al., Nucl. Phys. A523 (1991) 373.
65. A.F. Scott, et al., Univ. of Melborne School of Physics preprint UM-P-92/16 (1992).
66. M.E. Sevior, et al., Nucl. Phys. A454 (1986) 128.
67. E. Somorjai, et al., Astron. Astrophys. 333 (1998) 1112.
68. F.-K. Thielemann, M. Arnould, and J. W. Truran, in *Capture Gamma-Ray Spectroscopy*, eds. K. Abrahams, P. van Assche (IOP, Bristol 1988), p. 730.
69. P. Tischhauser, et al., Phys. Rev. Lett. 88 (2002) 072501.
70. J.K. Tuli, et al., Nuclear Wallet Cards, 5^{th} edition, Brookhaven National Laboratory, USA (1995); K.L. Kratz, et al., priv. comm.; F.-K. Thielemann, priv. comm.
71. P. Van Isacker, Phys. Rev. Lett., in press (2002).
72. T. A. Weaver and S. E. Woosley, Phys. Rep. 227 (1993) 65.
73. M. Wiescher and K.-U. Kettner, Astrophys. J. 263 (1982) 891.
74. R.R. Winters and R.L. Macklin, Astrophys. J. 329 (1988) 943.
75. S. E. Woosley, A. Heger, T. Rauscher, and R. D. Hoffman, Nucl. Phys. A, in press (2002).
76. S.E. Woosley and T.A. Weaver, Astrophys. J. Suppl. 101 (1995) 181.
77. P.R. Wrean, et al., Phys. Rev. C 49 (1994) 1205.